Antiviral Research 170 (2019) 104548

Contents lists available at ScienceDirect

Antiviral Research

journal homepage: www.elsevier.com/locate/antiviral

# Differing activities of oxysterol-binding protein (OSBP) targeting anti-viral compounds

Brett L. Roberts[a,1], Zachary C. Severance[a,1], Ryan C. Bensen[a], Anh T. Le-McClain[a], Cori A. Malinky[a], Evan M. Mettenbrink[a], Juan I. Nuñez[a], William J. Reddig[b], Earl L. Blewett[b], Anthony W.G. Burgett[a,*]

[a] Department of Chemistry and Biochemistry, University of Oklahoma, Norman, OK, United States
[b] Department of Biochemistry and Microbiology, Oklahoma State University Center for Health Sciences, Tulsa, OK, United States

A B S T R A C T

Oxysterol-binding Protein (OSBP) is a human lipid-transport protein required for the cellular replication of many types of viruses, including several human pathogens. The structurally-diverse small molecule compounds OSW-1, itraconazole (ITZ), T-00127-HEV2 (THEV) and TTP-8307 (TTP) inhibit viral replication through interaction with the OSBP protein. The OSW-1 compound reduces intracellular OSBP, and the reduction of OSBP protein levels persists multiple days after the OSW-1-compound treatment is stopped. The OSW-1-induced reduction of OSBP levels inhibited *Enterovirus* replication prophylactically in cells. In this report, the OSBP-interacting compounds ITZ, THEV, and TTP are shown not to reduce OSBP levels in cells, unlike the OSW-1-compound, and the OSW-1 compound is determined to be the only compound capable of providing prophylactic antiviral activity in cells. Furthermore, OSW-1 and THEV inhibit the binding of 25-hydroxycholesterol (25-OHC) to OSBP indicating that these compounds bind at the conserved sterol ligand binding site. The ITZ and TTP compounds do not inhibit 25-hydroxycholesterol binding to OSBP, and therefore ITZ and TTP interact with OSBP through other, unidentified binding sites. Co-administration of the THEV compound partially blocks the cellular activity of OSW-1, including the reduction of cellular OSBP protein levels; co-administration of the ITZ and TTP compounds have minimal effect on OSW-1 cellular activity further supporting different modes of interaction with these compounds to OSBP. OSW-1, ITZ, THEV, and TTP treatment alter OSBP cellular localization and levels, but in four distinct ways. Co-administration of OSW-1 and ITZ induced OSBP cellular localization patterns with features similar to the effects of ITZ and OSW-1 treatment alone. Based on these results, OSBP is capable of interacting with multiple structural classes of antiviral small molecule compounds at different binding sites, and the different compounds have distinct effects on OSBP cellular activity.

## 1. Introduction

Oxysterol-binding protein (OSBP) is a member of a lipid-binding protein family (i.e., OSBP and the OSBP-related proteins (ORPs)) conserved in all eukaryotes (Kentala et al., 2016; Pietrangelo and Ridgway, 2018). Originally discovered based on its high affinity binding to 25-hydroxycholesterol and other oxysterols, the cellular function of OSBP has long been associated with the sensing or the transport of lipids, particularly sterols (Kentala et al., 2016; Pietrangelo and Ridgway, 2018). All OSBP/ORP family members possess a C-terminal ~50 kDa OSBP-related ligand-binding domain (ORD) (Kentala et al., 2016; Pietrangelo and Ridgway, 2018). More recent work has identified OSBP as executing a critical lipid transport function at the membrane contact sites (MCS) between the ER and Golgi (Mesmin et al., 2013, 2017). OSBP transports cholesterol from the ER to the Golgi, while counter-transporting phosphosphoinositide-4-phosphate from the Golgi to the ER (Mesmin et al., 2013, 2017). In this role, OSBP mediates the necessary movement and regulation of the lipids between organelles, and OSBP is one of a growing roster of proteins, including multiple ORPs, involved in inter-organelle transport at MCS (Wong et al., 2019; Wang et al., 2019; Chung et al., 2015). ORP4 is the OSBP/ORP family member most closely related to OSBP based on conserved amino acid sequence (~64% overall sequence identity, ~67% in lipid binding domain) (Kentala et al., 2016; Pietrangelo and Ridgway, 2018). Despite their sequence similarity, OSBP and ORP4 perform different cellular functions (Kentala et al., 2016; Pietrangelo and Ridgway, 2018). In immortalized cell lines (Charman et al., 2014) and leukemia, ORP4 is highly expressed and drives proliferation (Zhong et al., 2016, 2019; Pan et al., 2018). In leukemia stem cells, ORP4 is recently reported to transfer phosphoinositide-2-phosphate ($PIP_2$) from the plasma membrane to PLCβ3 to trigger pro-growth cell signaling pathways (Pan et al., 2018; Zhong et al., 2019). In contrast, reduction of OSBP in cancer cells lines by >90% has no observable effect on cellular proliferation or morphology (Burgett et al., 2011; Roberts et al., 2019).

* Corresponding author.
*E-mail address:* anthony.burgett@ou.edu (A.W.G. Burgett).
[1] Co-first authors, contributed equally.

https://doi.org/10.1016/j.antiviral.2019.104548
Received 4 April 2019; Received in revised form 25 June 2019; Accepted 29 June 2019
Available online 02 July 2019
0166-3542/ 

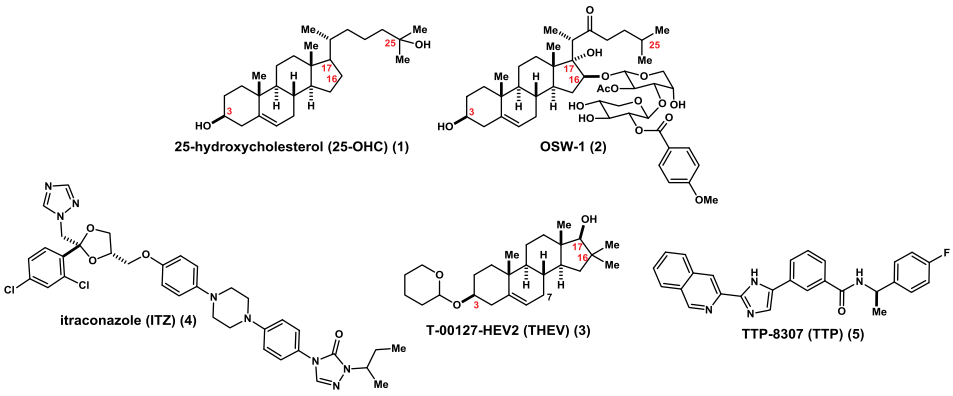


**Scheme 1. 25-Hydroxycholesterol and OSBP Interacting Antiviral Compounds.**

More recently, OSBP, but not ORP4, was determined to execute a critical role in the proliferation of RNA viruses (Strating et al., 2015a). This unexpected discovery was made through identifying OSBP as the cellular protein through which the compound itraconazole prevented broad spectrum *Enterovirus* viral replication (Strating et al., 2015b; Bauer et al., 2018). OSBP executes a vital role in the replication of a growing number of clinically-important human pathogens including *Enterovirus* genus pathogens (Strating et al., 2015a; Albulescu et al., 2015; Baggen et al., 2018), hepatitis C virus (HCV) (Amako et al., 2009, 2011), encephalomyocarditis virus (EMCV) (Dorobantu et al., 2016), dengue virus (Meutiawati et al., 2018), and Zika virus (Meutiawati et al., 2018). OSBP is important for the formation of the membrane bound viral replication organelles (RO), which form at the ER-Golgi interface (Nchoutmboube et al., 2015; Arita, 2014; Dorobantu et al., 2015).

Four antiviral compounds have been identified as functioning through targeting OSBP: OSW-1 (**2**) (Roberts et al., 2019; Albulescu et al., 2015), itraconazole (ITZ) (**3**) (Strating et al., 2015b; Bauer et al., 2018), T-00127-HEV-2 (THEV) (**4**) (Arita et al., 2013), and TTP-8307 (TTP) (**5**) (Arita et al., 2013) (Scheme 1). OSW-1 is an antiproliferative natural product compound that exerts its biological activity through interacting with OSBP and ORP4 (Burgett et al., 2011). The antiproliferative activity of the OSW-1 compound is likely due to interacting with ORP4, and the antiviral activity of OSW-1 is through its interaction with OSBP (Roberts et al., 2019; Strating et al., 2015a; Albulescu et al., 2015). ITZ, a clinically approved anti-fungal drug (Hitchcock, 1993), is a promiscuous binder reported to interact with VEGF2 (Chong et al., 2007; Nacev et al., 2011), Smoothened in the Hedgehog signaling pathway (Kim et al., 2010), and both VDAC1 and NPC1 simultaneously (Head et al., 2017). An additional report suggests that the ITZ antiviral activity is attributed to its interaction with the viral non-structural 3A protein in EV-A71, instead of OSBP (Gao et al., 2015).

There is no reported OSBP protein structure, but the conserved ORDs in related OSBP/ORP family members have been determined (Kentala et al., 2016; Pietrangelo and Ridgway, 2018; Wang et al., 2019). The solved ORP protein structures provide evidence for two OSBP small molecule ligand binding sites on the ORD: 1) a well-established oxysterol binding site (Im et al., 2005); and 2) a separate phospholipid binding site, distinct from the N-terminal Pleckstrin Homology (PH) domain, which also has the capacity to bind phosphoinositides (Wang et al., 2019; Tong et al., 2013a; Maeda et al., 2013). Functional studies have also demonstrated that the residues required for OSBP ORD phospholipid binding are not required for oxysterol binding (Mesmin et al., 2013, 2017; Tong et al., 2013b).

Of the four OSBP-interacting compounds, only OSW-1 (**2**) is established to effect binding to one of the two established OSBP ligand binding sites (i.e., oxysterol or phospholipid binding sites). OSW-1 (**2**) competitively inhibits the binding of 25-hydroxycholesterol (25-OHC) (**1**) to OSBP and ORP4 with low nanomolar $K_i$s (Burgett et al., 2011; Roberts et al., 2019). ITZ (**3**) is reported to have a $K_D$ of ~430 nM for full-length GFP-OSBP, as measured using microscale thermophoresis (Strating et al., 2015b). This method has not been used to measure binding of any other potential ligand to OSBP, including 25-OHC (**1**) or OSW-1 (**2**) (Strating et al., 2015a). OSBP binding measurements for THEV (**4**) and TTP (**5**) have not been reported. The antiviral activity of the THEV compound (**4**) is potentiated by OSBP knockdown in cells, which supports the compound targeting OSBP in cells (Arita et al., 2013). The TTP compound (**5**) is shown to inhibit the ability of OSBP to transport cholesterol between vesicles, *in vitro*. [26 13] Neither ITZ (**3**) or TTP (**5**) substantially inhibited the interaction of the N-terminal OSBP FFAT domain with the established OSBP-interacting protein VAP-A, as determined using bimolecular fluorescent complementation (BiMC) assay (Albulescu et al., 2017a). Based on these results, ITZ (**3**) or TTP (**5**) are inferred not to bind to the N-terminal of region of OSBP which contains the FFAT domain, but instead likely binds to the C-terminal ORD (Albulescu et al., 2017a). Lipid transfer assays using OSBP proteolyzed fragments suggested that ITZ interacted with the C-terminal ORD and blocked the ORD transfer activity of both sterols and PI4P (Albulescu et al., 2017b). ITZ was computationally docked into a homology structure of the OSBP ORD overlapping with the putative oxysterol binding site (Bauer et al., 2018). OSW-1 (**2**), ITZ (**3**), THEV (**4**), and TTP (**5**) have minimal overall structural similarity (Scheme 1), although THEV and OSW-1 share a steroidal core.

OSW-1 treatment induces a pronounced and lasting reduction in cellular OSBP levels (Burgett et al., 2011; Roberts et al., 2019). A short duration (1–6 h), non-cytotoxic dose of OSW-1 reduces OSBP levels in cells >90%, and the reduction of cellular OSBP levels persists multiple days after the compound treatment ceased (Roberts et al., 2019). The cells with OSBP levels reduced >90% for multiple days show no effect on cellular proliferation, viability, or morphology (Roberts et al., 2019). Cellular treatment with the OSBP high affinity ligands 25-OHC or the natural product schweinfurthin A compound do not reduce OSBP levels, indicating that a reduction of cellular OSBP levels is not a universal response to ligand binding (Burgett et al., 2011). Furthermore, the OSW-1-induced reduction of OSBP levels in cells confers prophylactical antiviral activity against multiple *Enterovirus* strains 24 h after the end of compound treatment (Roberts et al., 2019).

In this report, the other antiviral OSBP-interacting compounds ITZ, THEV, and TTP are shown not to reduce OSBP levels in cells or to provide prophylactic antiviral activity. Additionally, the THEV compound is shown to inhibit the binding of 25-OHC to OSBP and to ORP4, similar to OSW-1. ITZ and TTP do not inhibit 25-OHC binding to OSBP and ORP4, suggesting these compounds interact with OSBP through a different binding site. ITZ and THEV at high concentrations relative to OSW-1 can partially block the OSBP reduction caused by OSW-1. Interestingly, all four compounds—OSW-1, ITZ, THEV, and TTP—produce distinct changes on OSBP localization in cells. These

results indicate that the structurally-diverse antiviral small molecule compounds are capable of interacting with and modulating the OSBP cellular activity through multiple different modes of action.

## 2. Materials and methods

### 2.1. Cell lines and viruses

HCT-116, HEK293, RD, and HeLa cell lines were purchased from ATCC. HEK293 STF (CRL-3249), RD (CCL-136), and HeLa (CCL-2) were cultured in DMEM (Thermo 11995073) supplemented with 10% Hyclone (Fisher Sci SH3006603) and 1% penicillin streptomycin (Thermo 15140122). HCT-116 (ATCC CCL-247) was cultured in McCoys 5A media (Thermo 16600108) supplemented with 10% Hyclone and 1% penicillin streptomycin. Coxsackievirus A9 (strain CoxA9-01) and Echovirus 2 (strain Echo2-01) were obtained from the Oklahoma State Department of Health Laboratory.

### 2.2. Western blotting antibodies

Primary antibodies used for Western blot were OSBP A-5 (Santa Cruz sc-365,771) and Beta-actin HRP (Santa Cruz sc-47778 HRP). Secondary antibodies used were goat anti-mouse $IgG_1$-HRP (Santa Cruz sc-2060).

### 2.3. Immunofluorescent imaging antibodies

Primary antibodies used for immunofluorescent (IF) imaging were OSBP1 1F2 (Novus NBP2-00935) and TGN46 (Novus NBP1-49643). Secondary IF antibodies used were goat anti-mouse IgG H&L Alexa Fluor® 488 (Abcam ab150113) and donkey anti-rabbit IgG H&L Alexa Fluor® 594 (Abcam ab150076).

### 2.4. OSW-1, ITZ, THEV, and TTP compounds

OSW-1 was generated either through chemical synthesis in our lab (Yu and Jin, 2002) or isolation from the natural source (Mimaki et al., 1997). ITZ was purchased from Sigma-Aldrich (I6657) as a 1:1:1:1 mixture of diastereomer. Both the T-00127-HEV2 (THEV) and TTP-8307 (TTP) compounds were synthesized in our group. TTP-8307 was made following the published routes (Albulescu et al., 2017a). To our knowledge, a procedure for the synthesis of the THEV compound had not been reported. OSW-1, THEV, and TTP were subjected to HPLC purification to produce analytically pure compounds (>95% purity) and fully characterized using spectroscopic techniques (see Supporting Information for compound data).

### 2.5. OSBP expression in cells upon compound treatments

HCT-116 or HEK293 cells were seeded out $5 \times 10^5$ into 6-well plates and incubated at 37 °C for 20 h. Compound stock solutions were diluted in complete media before treating the cells (1 nM OSW-1 and/or 10,000 nM THEV, TTP, ITZ). After compound treatment, cells were lysed according to the lysis procedure in the Supporting Information.

### 2.6. Viral proliferation assays

The CoxA9-01 or Echo2-01 clinically isolated viruses were passaged twice in RD cells and then stored at −80 °C until use.

*Continual Compound Treatment Antiviral Experiment:* $2.0 \times 10^5$ HeLa cells were plated in 1 mL of media in 24-well plates and incubated overnight. Then, the media was removed, and cells were infected with either CoxA9-01 or Echo2-01 viruses (estimated MOI = 1.0) in serum-free DMEM. The virus and cells were incubated for 30 min, at which point the virus inoculum was removed, and the culture was washed once with serum free media. Then, the infected cells were dosed with the indicated compound, 10,000 nM for THEV, TTP, and ITZ, or 10 nM for OSW-1 (4 treatments per virus for each compound) in 1 mL of complete media, and incubated with the compound for 10 h, and then snap-frozen and stored at −80 °C until processing. Viral titration was performed by thawing the plates, scraping the cells into micro-centrifuge tubes, and then centrifuging the samples at 10,000 g at 4 °C to produce the virus containing supernatant, which is assayed for TCID-50 titration on subconfluent RD cells (N = 3). The graphs represent averages of three independent experiments.

*Compound Washout Antiviral Experiment:* This experiment was performed identically to the antiviral assay described above, with the following changes. Cells were treated with the indicated compound-containing media for 6 h. Then, the cells were washed three times in compound-free complete media and incubated for 24 h in compound-free media. After 24 h washout recovery, the cells were then infected with CoxA9-01 or Echo2-01 viruses at an estimated MOI of 1.0 for 30 min, cultured for 10 h in complete media, and then subjected to analysis as described above. There were four treatments per virus for each compound, n = 4. The graphs represent three independent experiments.

### 2.7. 96-Well [3H]-25-OHC competitive binding assay

The [3H]-25-OHC binding assay was conducted as previously described (Burgett et al., 2011; Roberts et al., 2019).

### 2.8. Viability assays

*96-well Cytotoxicity Assay:* 48 h cytotoxicity assays were performed in 96-well plates using standard CellTiter-Blue® (Promega) procedure. See supporting Information for a detailed protocol.

*Trypan Blue Cell Viability Assay-* HCT-116 cells were seeded out $5 \times 10^5$ into 6 well plates incubated at 37 °C for 20 h. The cells were treated with DMSO 1 nM OSW-1, 10,000 nM Itraconazole, 10,000 nM TTP, 10,000 nM THEV, or a combination of treatments for 24 h. Cells were washed once with PBS, detached using TrypLE™ Express trypsin, and counted on a TC20™ Automated Cell Counter (BioRad) by combining 10 μL of cell solution with 10 μL Trypan Blue stain (Thermo 15250061).

### 2.9. Immunofluorescence cell imaging experiments

HCT-116 immunofluorescent microscopy on endogenous OSBP was performed as described previously (Roberts et al., 2019), except with a 24 h compound treatment.

### 2.10. Statistical analysis

All results are expressed as mean ± SD and are $n \geq 3$ unless otherwise stated. All statistical tests were performed using GraphPad Prism 7.0. Comparison between groups was made by using a one-way ANOVA with a follow up Dunnett's test. The p values are reported using GraphPad Prism: *$p \leq 0.05$, **$p \leq 0.01$ ***$p \leq 0.001$, and ****$p \leq 0.0001$.

### 2.11. Other methods

Any remaining experimental procedures and additional details of the methods outlined above are described in the Supporting Information.

## 3. Results

### 3.1. Only OSW-1, and not ITZ, THEV, or TTP, reduce OSBP levels in cells

OSW-1 treatment is established to reduce OSBP cell levels in multiple cells lines, including HEK293, HCT-116, and HeLa (Burgett et al.,

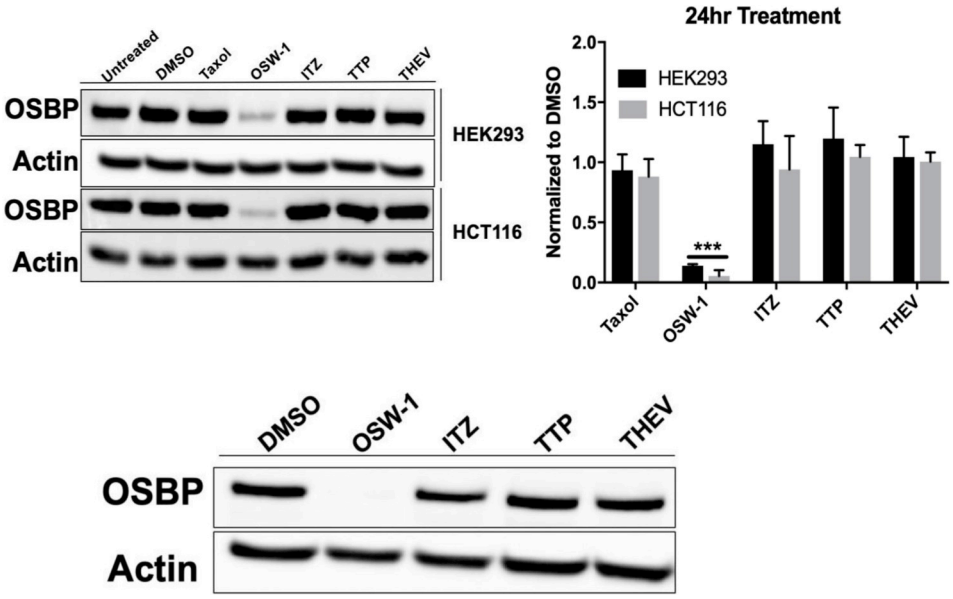


**Fig. 1. OSW-1 is the Only Compound That Reduces Cellular OSBP Levels.** A) Effect of compound treatment on cellular OSBP expression in HCT-116 and HEK293 cells. Cells were treated with DMSO vehicle control, OSW-1 (1 nM), Taxol (10 nM), ITZ (10,000 nM), TTP (10,000 nM) or THEV (10,000 nM) for 24 h. Representative Western blot and average of multiple independent experiments shown. **B)** OSBP levels via Western blot in HeLa cells treated with compound (OSW-1 10 nM, THEV 10,000 nM, ITZ 10,000 nM, or TTP 10,000 nM) for 6 h followed by cell washing and incubation in compound-free media for 24 h. Western blot represents OSBP protein levels at the time of inoculation during washout treatment in antiviral experiments (see Fig. 2).

2011; Roberts et al., 2019). HEK293 and HCT-116 cells treated with 1 nM of the OSW-1 compound for 24 h show the pronounced reduction of OSBP cellular levels (Fig. 1A). (Burgett et al., 2011; Roberts et al., 2019) 10,000 nM treatment of the cells for 24 h with the ITZ, THEV, or TTP compounds do not reduce OSBP levels. Taxol, the tubulin binding anticancer drug, is included to show that OSBP levels are not reduced upon cellular treatment with a cytotoxic compound. 25-OHC also does not reduce OSBP levels in cells (Burgett et al., 2011). OSW-1 is also the only compound to induce the reduction of OSBP in levels in HeLa cells after 6 h treatment and 24 h of compound-free recovery (Fig. 1B); ITZ, THEV, and TTP at 10,000 nM treatment did not affect OSBP levels after the 6 h treatment, 24 h recovery (Fig. 1B).

### 3.2. Only OSW-1, and not ITZ, THEV, or TTP, induces prophylactic antiviral activity in cells

Treatment of cells with 1 nM OSW-1 for 6 h, followed by removing the compound from the cells triggers a repression of OSBP levels that last for 72 h after the compound treatment is stopped (Roberts et al., 2019). Previously, a 1 nM OSW-1 treatment in HeLa cells conferred significant antiviral protection against the *Enterovirus* pathogens Cosackievirus 9a or Echovirus 2 24 h after OSW-1 treatment ended (Roberts et al., 2019). The ITZ, THEV, and TTP compounds were tested for prophylactic antiviral activity similar to that of OSW-1 (Fig. 2). Cells infected with virus for 30 min, followed by a 10 h treatment with OSW-1 (10 nM), ITZ (10,000 nM), THEV (10,000 nM) or TTP (10,000 nM) (Fig. 2A) showed antiviral activity consistent with previous reports (Roberts et al., 2019; Strating et al., 2015b; Albulescu et al., 2015, 2017a; Arita et al., 2013). However, OSW-1 is the only compound that displayed antiviral activity when viral infection occurred 24 h after compound treatment stopped (Fig. 2B). Cellular OSBP levels are reduced >90% after the 6 h OSW-1 treatment, 24 h recovery, which is just prior to viral infection (Fig. 1B). 6 h OSW-1 treatment of cells is not cytotoxic nor anti-proliferative (Roberts et al., 2019).

### 3.3. Both OSW-1 and THEV inhibit oxysterol binding to OSBP and ORP4; ITZ and TTP do not

OSW-1, ITZ, THEV, and TTP were tested in the established 96-well OSBP competition ligand binding assay, which measures compound binding to OSBP through inhibition of 25-OHC binding (Burgett et al., 2011; Roberts et al., 2019). $K_D$ of 25-OHC binding to human OSBP is

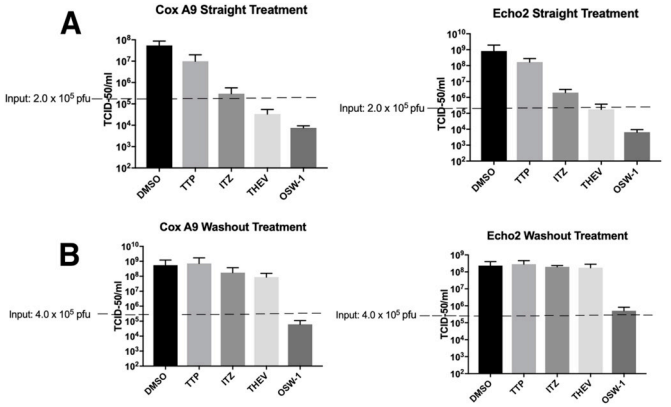


**Fig. 2. OSW-1 is the Only Compound That Provides Prophylactic Anti-Viral Activity.** A) HeLa cells were infected with either Cosackievirus A9 or Echovirus 2 for 30 min, followed by compound treatment for 10 h OSW-1 (10 nM), THEV (10,000 nM), ITZ (10,000 nM), or TTP (10,000 nM). **B)** Compound Prophylactic Antiviral Activity. HeLa cells were treated with OSW-1 (10 nM), THEV (10,000 nM), ITZ (10,000 nM), or TTP (10,000 nM) for 6hr. Compound was removed from the cells and cell media, and the cells were incubated in compound-free media for 24 h. Then, cells were infected with Cosackievirus A9 or Echovirus 2 for 30 min, followed by 10 h incubation in compound-free media. Viral titers from three independent experiments shown.

22 ± 5 nM (Supp. Fig 2); human ORP4 25-OHC $K_D$ is reported as 54 ± 23 nM (Burgett et al., 2011). Compounds were measured for inhibition of binding of 20 nM of $^3$H-25-OHC to either OSBP or ORP4 overexpressed in HEK239T lysate. Consistent with published reports, OSW-1 produced a $K_i$ in this binding assay of 16 ± 4 nM for OSBP and 71 ± 6 for ORP4 (Fig. 3). (Burgett et al., 2011; Roberts et al., 2019) The THEV compound also showed strong competitive binding of 25-OHC, with $K_i$s of 22 ± 15 nM against OSBP and 98 ± 15 nM for ORP4 (Fig. 3). ITZ and TTP showed no 25-OHC inhibition binding to OSBP or ORP4 at a concentration of 10,000 nM (Fig. 3).

### 3.4. THEV and ITZ, but not TTP, inhibits OSW-1 activity in cells supporting different modes of compound binding to OSBP

Treatment of HCT-116 cells with 1 nM of OSW-1 and 10,000 nM ITZ shows a slight (~15–20%) effect on cell population after 24 h, assessed

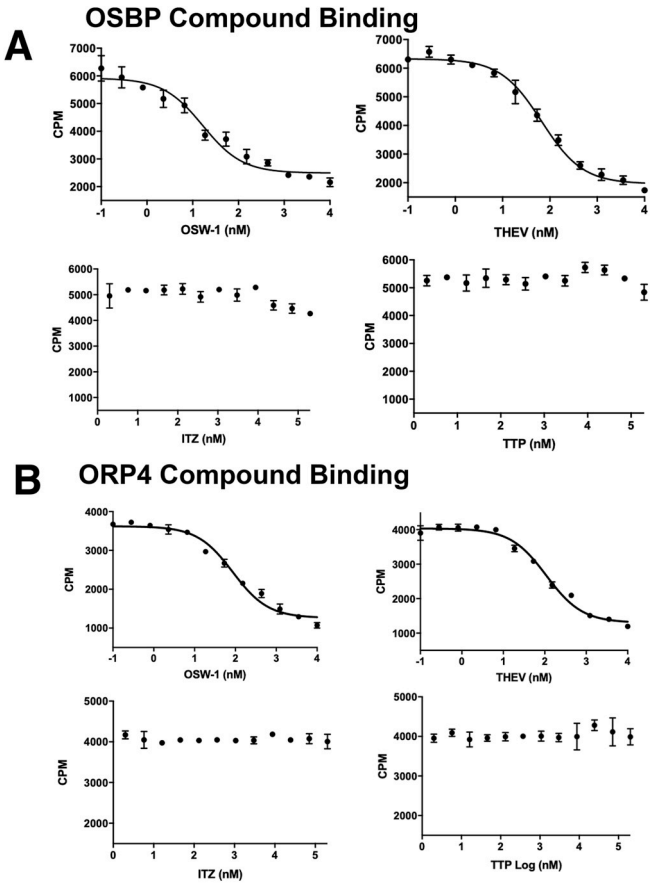


C

| Compound | OSBP $K_i$ (nM) | ORP4 $K_i$ (nM) |
|---|---|---|
| OSW-1 | 16 ± 4 | 71 ± 6 |
| THEV | 22 ± 15 | 98 ± 14 |
| Itraconazole | - | - |
| TTP | - | - |

**Fig. 3. OSW-1 and THEV Inhibit 25-OHC Binding to OSBP; ITZ and TTP Do Not.** Compound binding to OSBP (**A**) or ORP4 (**B**) measured using a competitive 25-OHC binding assay. Representative inhibition binding curves are shown. **C**) Average $K_i$ values from three independent binding experiments for OSW-1 and THEV to OSBP and ORP4. ITZ and TTP show no 25-OHC competitive binding.

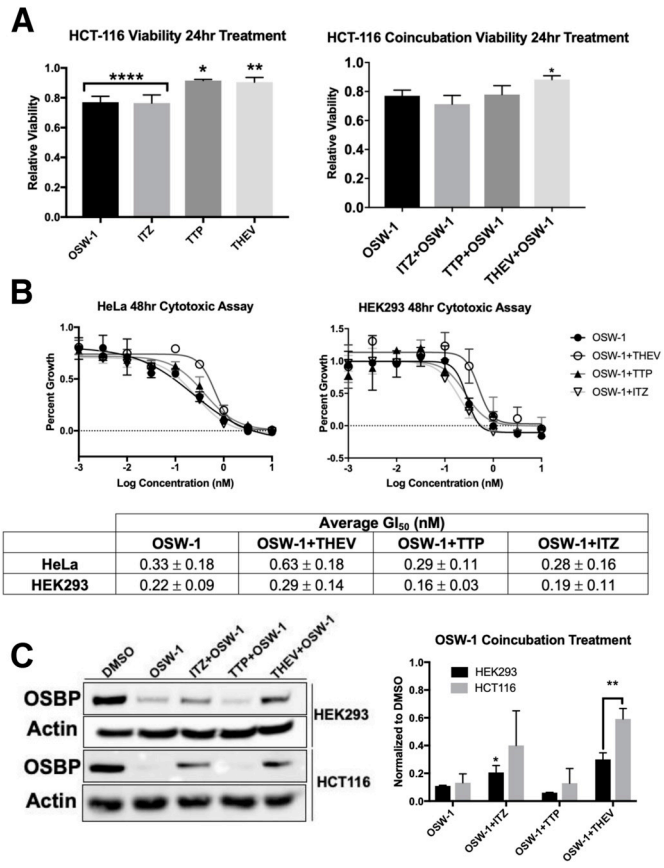


| | Average $GI_{50}$ (nM) | | | |
|---|---|---|---|---|
| | OSW-1 | OSW-1+THEV | OSW-1+TTP | OSW-1+ITZ |
| HeLa | 0.33 ± 0.18 | 0.63 ± 0.18 | 0.29 ± 0.11 | 0.28 ± 0.16 |
| HEK293 | 0.22 ± 0.09 | 0.29 ± 0.14 | 0.16 ± 0.03 | 0.19 ± 0.11 |

**Fig. 4. THEV Co-administration blocks the cellular activity of OSW-1.** A) Viability of cells using Trypan Blue stain after 24 h of compound treatment or co-administration of OSW-1 (1 nM) with 10,000 nM of ITZ, THEV, or TTP. **B)** Cytotoxicity of 1 nM OSW-1 at 48 h co-administered with 10,000 nM THEV, TTP, or ITZ in HCT-116 and HEK293 cells. Representative cytotoxicity curves and average $GI_{50}$ of three independent experiments shown. **C)** OSBP levels in HCT-116 and HEK293 cells of co-administration of 1 nM of OSW-1 with 10,000 nM of ITZ, THEV or TTP for 24 h. Representative Western blot and average of three independent experiments shown.

through cell counting after Trypan blue staining (Fig. 4A). 10,000 nM of THEV or TTP treatment does not affect the cell population (Fig. 4A). Co-administration of 1 nM OSW-1 with 10,000 nM of either ITZ, TTP, or THEV shows that OSW-1 and ITZ do not additively reduce the cell population (Fig. 4A). Co-administration of 10,000 nM of THEV with OSW-1 rescues cell population numbers (Fig. 4A). Extended cellular treatment with OSW-1 longer than 24 h is antiproliferative in immortalized cell lines, as determined using assays for cell metabolic activity (Burgett et al., 2011; Roberts et al., 2019). In a 48 h assay for cell metabolic activity, ITZ, THEV, and TTP showed no antiproliferative activity at $<10{,}000$ nM concentrations (Fig. 4B, Supp. Fig. 1). OSW-1 produced a growth inhibition 50% ($GI_{50}$) value of 0.33 ± 0.18 nM in HeLa cells and 0.22 ± 0.09 nM in HEK293 cells after 48 h treatment. Co-administering either ITZ, THEV, or TTP at 10,000 nM does not significantly affect the antiproliferative OSW-1 activity in either HeLa or HEK293 cells (Fig. 4B). Co-administration of either 10,000 nM THEV or ITZ with 1 nM OSW-1 partially blocks the reduction of OSBP levels in both HEK293 and HCT116 cells (Fig. 4C). THEV rescues OSBP levels to a greater extent than ITZ (Fig. 4C). Co-administration of 10,000 nM of TTP with 1 nM OSW-1 has no effect on OSBP levels in cells (Fig. 4C).

### *3.5. OSW-1, ITZ, THEV, and TTP treatments alter OSBP localization in cells in different ways*

OSBP localization patterns in cells are known to be altered by ligand binding, including through interacting with oxysterols (Mesmin et al., 2013; Burgett et al., 2011; Ridgway et al., 2008), OSW-1[12,13,37], ITZ (Strating et al., 2015a; Albulescu et al., 2017a), THEV (Arita et al., 2013), and TTP (Albulescu et al., 2017a). HCT-116 cells have been used for OSBP localization experiments previously (Burgett et al., 2011; Roberts et al., 2019). In HCT-116 cells, endogenous OSBP is largely localized with the Golgi marker in a diffused perinuclear pattern (Fig. 5A), which is consistent with OSBP localization in the ER/Golgi MCS (Mesmin et al., 2013). Treatment with 10,000 nM of 25-OHC for 24 h strongly colocalizes OSBP with the Golgi marker in a small area. 1 nM OSW-1 treatment for 24 h causes a significant reduction of cellular OSBP levels as expected based on the Western blot results (Roberts et al., 2019), and the remaining OSBP is tightly grouped around one location, possibly large vesicles. The Golgi marker in the OSW-1-treated cells is diffused and punctate in appearance (Fig. 5A). 10,000 nM of ITZ treatment causes OSBP to adopt a more punctate pattern closely associated with the Golgi marker, although the Golgi marker shows more diffused cytoplasm signal (Fig. 5A). 10,000 nM of TTP treatment induces a tight colocalization of OSBP with the Golgi marker with a perinuclear pattern close to the vehicle (DMSO) treated cell (Fig. 5A). 10,000 nM of THEV treatment induces OSBP localization to confined

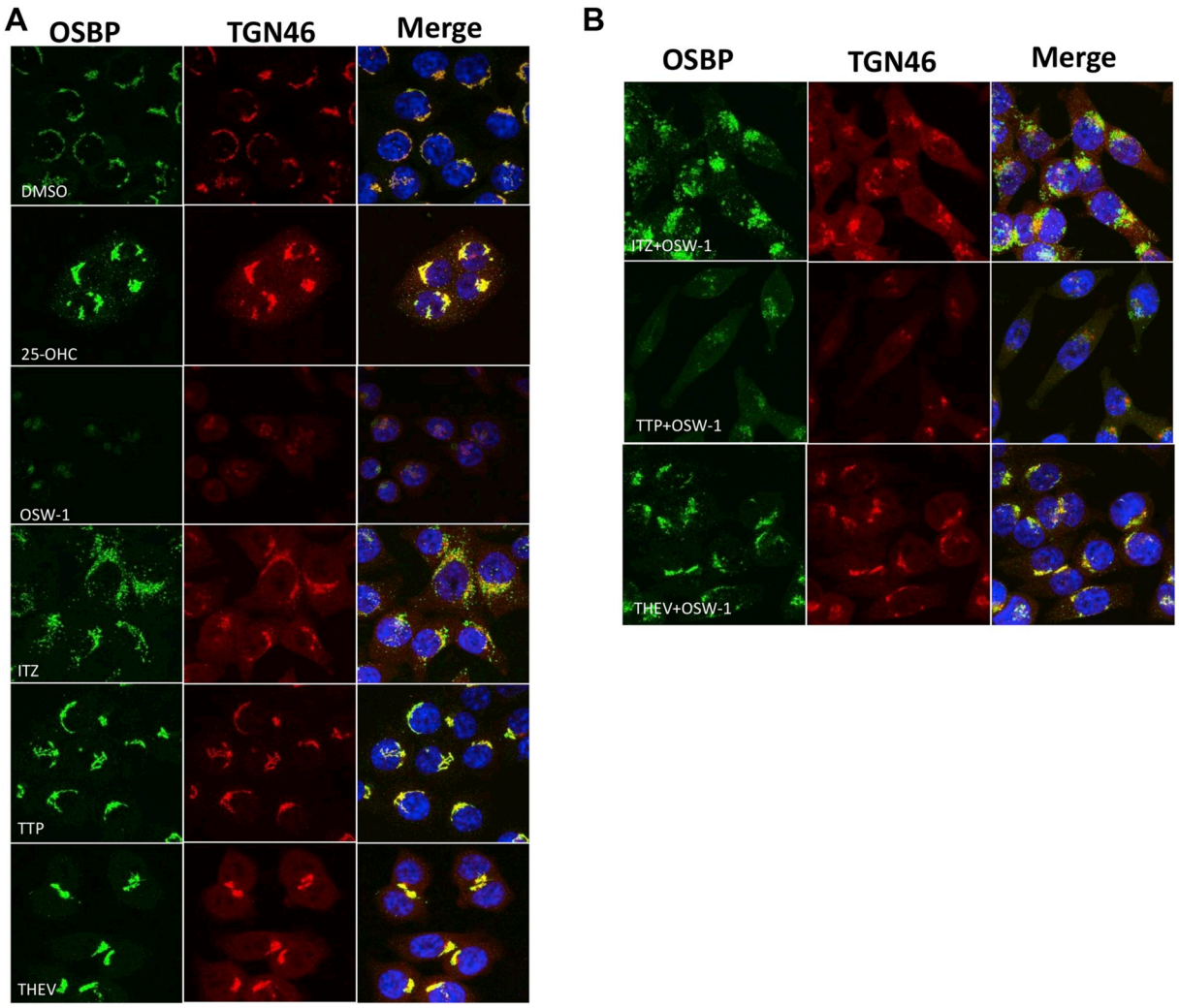


**Fig. 5. OSW-1, THEV, ITZ, and TTP Cellular Treatment All Have Distinct Effects on OSBP Cellular Localization.** A) Immunofluorescent confocal microscopy of HCT-116 cells treated for 24 h with either DMSO (vehicle), 10,000 nM 25-OHC, 1 nM OSW-1, 10,000 nM ITZ, 10,000 nM TTP, or 10,000 nM THEV. OSBP shown in green; Golgi marker TGN46 shown in red; nucleus stain in blue. The merged images indicates colocalization of the OSBP and Golgi marker. **B)** Co-administration of 1 nM OSW-1 with 10,000 nM ITZ, 10,000 nM TTP, or 10,000 nM THEV.

area tightly packed with the Golgi marker, very similar to 25-OHC treatment (Fig. 5A).

The effects of co-administration of OSW-1 with the other compounds shows that ITZ and THEV alter the OSW-1-induced OSBP localization pattern (Fig. 5B). Co-administration of 1 nM of OSW-1 with 10,000 nM of ITZ produces a tight localization of OSBP with a stronger signal than OSW-1 alone (Fig. 5A and B). The Golgi marker in the OSW-1 + ITZ treated cells is weakly diffused through the cytoplasm, similar to ITZ alone (Fig. 5A). Overall, the cellular effects of OSW-1 + ITZ treatment is a hybrid of the effects of separate treatment of OSW-1 and ITZ, except for stronger OSBP signal (Fig. 5A and B). Similarly, co-administration of 1 nM of OSW-1 with 10,000 nM of THEV produces cellular localization effects with elements of both OSW-1 and THEV treatment alone (Fig. 5A and B). The OSW-1 + THEV and OSW-1 + ITZ treated cells possess more OSBP than the OSW-1 alone cells, verifying that THEV and ITZ can block the reduction in OSBP levels, as shown via Western blot (Fig. 4C). Similar to THEV treatment alone (Fig. 5A), the OSW-1 + THEV treatment includes significant colocalization of OSBP with the Golgi marker, although the colocalization pattern is not as tight as with THEV alone (Fig. 5B). The OSW-1 + TTP treated cells show low expression of OSBP with a pattern not consistent with the OSW-1 alone or TTP alone treatment.

## 4. Discussion

The results show that the identified OSBP small molecule ligands (i.e., OSW-1, ITZ, THEV, and TTP) do not interact with OSBP through a common binding site and do not have identical effects on OSBP in cells. OSW-1 is the only compound that: 1) causes a reduction in cellular OSBP levels (Fig. 1), and, 2) induces a prophylactic antiviral response in cells (Fig. 2B). These results suggest that it is the reduction of OSBP levels that confers the prophylactic antiviral activity. OSW-1 and THEV both compete with high affinity for 25-OHC binding to OSBP, suggesting that OSW-1 and THEV likely have the same or overlapping OSBP binding sites. Both OSW-1 and THEV possess a steroidal structure, although, importantly, THEV lacks the sterol side chain (Scheme 1). The ability of both OSW-1 and THEV to show high affinity interactions with OSBP and ORP4, as determined through $K_i$ values, suggests the sterol component of OSW-1 and THEV is responsible for OSBP binding, and that the reduction of OSBP levels by OSW-1 is likely caused by the disaccharide portion of the compound.

Interestingly, neither ITZ or TTP inhibit 25-OHC binding to OSBP or ORP4. This suggests these two compounds, if they directly interact with OSBP, have binding sites separate from the sterol binding site. These results, in combination with previous reports, suggest that ITZ and TTP

interact with C-terminal OSBP-related ligand-binding domain (i.e, ORD) at locations that do not effect oxysterol binding.

THEV substantially inhibits the activity of OSW-1 in cells, albeit at much higher relative concentrations (i.e.,1 nM OSW-1 vs. 10,000 nM THEV) (Fig. 4A, B, 4C and Fig. 5B), confirming the overlapping OSBP binding between OSW-1 and THEV. The requirement for much higher THEV concentration in cells to counter OSW-1 activity could be the result of: 1) THEV's low specificity and multiple binding partners in cells; 2) poor cellular uptake of THEV in cells from the culture media, or 3) a high rate of cellular metabolism of the THEV compound. Similar to THEV, 25-OHC is commonly administered to cells at micromolar concentrations to affect OSBP, despite a low nanomolar 25-OHC OSBP $K_D$ (Fig. 5A). (Burgett et al., 2011; Ridgway et al., 1992) The tetrahydropyran acetal group on the 3-hydroxyl sterol position of THEV is expected to be labile under the acidic aqueous conditions likely encountered in cells, which could lead to degradation of the compound into an inactive form.

Co-administration of ITZ does somewhat prevent the reduction of OSBP levels induced by OSW-1 (Fig. 4C), and co-administration of ITZ and OSW-1 produces an OSBP cellular localization pattern that appears to have features in common with both OSW-1 and ITZ. These initial results suggest the possibility that OSBP might be capable of interacting with both OSW-1 and ITZ at different binding sites simultaneously. Interestingly, TTP did not alter the activity of OSW-1 in cells (Fig. 4A, B, 4C), although TTP co-administered with OSW-1 does induce a different OSBP localization pattern (Fig. 5B). These results suggest that TTP could have a modality of OSBP binding different than ITZ, indicating possibly a second, non-sterol binding site on the OSBP C-terminal domain. In aggregate, these results reveal OSBP to be able to bind multiple, structurally-diverse compounds through different binding sites to induce different biological activities. Therefore, the different OSBP targeting compounds can be used to potentially define different aspects of OSBP biology and present an array of modes for potential antiviral drug development through targeting OSBP.

## Acknowledgements

Thanks to the following funding sources: OCAST Health Grant HR17-116; NIH NCI: Innovation Molecular Analysis Technologies (IMAT) Program R21CA204706 (Burgett PI); NIH NIGMS R01GM116116; and the Barnes Family Foundation (Tulsa, Oklahoma). The laboratories of E. Zgurskaya and A. Duerfeldt are thanked for the use of laboratory equipment.

## Appendix A. Supplementary data

Supplementary data to this article can be found online at https://doi.org/10.1016/j.antiviral.2019.104548.

## References

Albulescu, L., Strating, J.R.P.M., Thibaut, H.J., Van Der Linden, L., Shair, M.D., Neyts, J., Van Kuppeveld, F.J.M., 2015. Broad-range inhibition of Enterovirus replication by OSW-1, a natural compound targeting OSBP. Antivir. Res. 117, 110–114.

Albulescu, L., Bigay, J., Biswas, B., Weber-Boyvat, M., Dorobantu, C.M., Delang, L., van der Schaar, H.M., Jung, Y.-S., Neyts, J., Olkkonen, V.M., et al., 2017Aa. Uncovering oxysterol-binding protein (OSBP) as a target of the anti-enteroviral compound TTP-8307. Antivir. Res. 140, 37–44.

Albulescu, L., Bigay, J., Biswas, B., Weber-Boyvat, M., Dorobantu, C.M., Delang, L., van der Schaar, H.M., Jung, Y.-S., Neyts, J., Olkkonen, V.M., et al., 2017Ab. Uncovering oxysterol-binding protein (OSBP) as a target of the anti-enteroviral compound TTP-8307. Antivir. Res. 140, 37–44.

Amako, Y., Sarkeshik, A., Hotta, H., Yates, J., Siddiqui, A., 2009. Role of oxysterol binding protein in hepatitis C virus infection. J. Virol. 83 (18), 9237–9246.

Amako, Y., Syed, G.H., Siddiqui, A., 2011. Protein kinase D negatively regulates hepatitis C virus secretion through phosphorylation of oxysterol-binding protein and ceramide transfer protein. J. Biol. Chem. 286 (13), 11265–11274.

Arita, M., 2014. Phosphatidylinositol-4 kinase III Beta and oxysterol-binding protein accumulate unesterified cholesterol on poliovirus-induced membrane structure. Microbiol. Immunol. 58 (4), 239–256.

Arita, M., Kojima, H., Nagano, T., Okabe, T., Wakita, T., Shimizu, H., 2013. Oxysterol-binding protein family I is the target of minor enviroxime-like compounds. J. Virol. 87 (8), 4252–4260.

Baggen, J., Thibaut, H.J., Strating, J.R.P.M., van Kuppeveld, F.J.M., 2018. The life cycle of non-polio enteroviruses and how to target it. Nat. Rev. Microbiol. 16 (6), 368–381.

Bauer, L., Ferla, S., Head, S.A., Bhat, S., Pasunooti, K.K., Shi, W.Q., Albulescu, L., Liu, J.O., Brancale, A., Kuppeveld, F. J. M. Van, et al., 2018. Structure-activity relationship study of itraconazole , a broad-range inhibitor of picornavirus replication that targets oxysterol-binding protein (OSBP). Antivir. Res. 156, 55–63.

Burgett, A.W.G., Poulsen, T.B., Wangkanont, K., Anderson, D.R., Kikuchi, C., Shimada, K., Okubo, S., Fortner, K.C., Mimaki, Y., Kuroda, M., et al., 2011. Natural products reveal cancer cell dependence on oxysterol-binding proteins. Nat. Chem. Biol. 7 (9), 639–647.

Charman, M., Colbourne, T.R., Pietrangelo, A., Kreplak, L., Ridgway, N.D., 2014. Oxysterol-binding protein (OSBP)-Related protein 4 (ORP4) is essential for cell proliferation and survival. J. Biol. Chem. 289 (22), 15705–15717.

Chong, C.R., Xu, J., Lu, J., Bhat, S., Sullivan, D.J., Liu, J.O., 2007. Inhibition of angiogenesis by the antifungal drug itraconazole. ACS Chem. Biol. 2 (4), 263–270.

Chung, J., Torta, F., Masai, K., Lucast, L., Czapla, H., Tanner, L.B., Narayanaswamy, P., Wenk, M.R., Nakatsu, F., De Camilli, P., 2015. PI4P/Phosphatidylserine countertransport at ORP5- and ORP8-mediated ER-plasma membrane contacts. Science (80-. ) 349 (6246), 428–432.

Dorobantu, C.M., Albulescu, L., Harak, C., Feng, Q., van Kampen, M., Strating, J.R.P.M., Gorbalenya, A.E., Lohmann, V., van der Schaar, H.M., van Kuppeveld, F.J.M., 2015. Modulation of the host lipid landscape to promote RNA virus replication: the picornavirus encephalomyocarditis virus converges on the pathway used by hepatitis C virus. PLoS Pathog. 11 (9) e1005185.

Dorobantu, C.M., Albulescu, L., Lyoo, H., van Kampen, M., De Francesco, R., Lohmann, V., Harak, C., van der Schaar, H.M., Strating, J.R.P.M., Gorbalenya, A.E., et al., 2016. Mutations in encephalomyocarditis virus 3A protein uncouple the dependency of genome replication on host factors phosphatidylinositol 4-kinase IIIα and oxysterol-binding protein. mSphere 1 (3) e00068-16.

Gao, Q., Yuan, S., Zhang, C., Wang, Y., Wang, Y., He, G., Zhang, S., Altmeyer, R., Zou, G., 2015. Discovery of itraconazole with broad-spectrum in vitro antienterovirus activity that targets nonstructural protein 3A. Antimicrob. Agents Chemother. 59 (5), 2654–2665.

Head, S.A., Shi, W.Q., Yang, E.J., Nacev, B.A., Hong, S.Y., Pasunooti, K.K., Li, R.-J., Shim, J.S., Liu, J.O., 2017. Simultaneous targeting of NPC1 and VDAC1 by itraconazole leads to synergistic inhibition of MTOR signaling and angiogenesis. ACS Chem. Biol. 12 (1), 174–182.

Hitchcock, C.A., 1993. Resistance of Candida albicans to azole antifungal agents. Biochem. Soc. Trans. 21 (4), 1039–1047.

Im, Y.J., Raychaudhuri, S., Prinz, W. a, Hurley, J.H., 2005. Structural mechanism for sterol sensing and transport by OSBP-related proteins. Nature 437 (7055), 154–158.

Kentala, H., Weber-Boyvat, M., Olkkonen, V.M., 2016. OSBP-related protein family: mediators of lipid transport and signaling at membrane contact sites. In: International Review of Cell and Molecular Biology, vol. 321. Elsevier Inc., pp. 299–340.

Kim, J., Tang, J.Y., Gong, R., Kim, J., Lee, J.J., Clemons, K.V., Chong, C.R., Chang, K.S., Fereshteh, M., Gardner, D., et al., 2010. Itraconazole, a commonly used antifungal that inhibits Hedgehog pathway activity and cancer growth. Cancer Cell 17 (4), 388–399.

Maeda, K., Anand, K., Chiapparino, A., Kumar, A., Poletto, M., Kaksonen, M., Gavin, A., 2013. Interactome map uncovers phosphatidylserine transport by oxysterol-binding proteins. Nature 501 (7466), 257–261.

Mesmin, B., Bigay, J., Moser von Filseck, J., Lacas-Gervais, S., Drin, G., Antonny, B., 2013. A four-step cycle driven by PI(4)P hydrolysis directs sterol/PI(4)P exchange by the ER-golgi tether OSBP. Cell 155 (4), 830–843.

Mesmin, B., Bigay, J., Polidori, J., Jamecna, D., Lacas-Gervais, S., Antonny, B., 2017. Sterol transfer, PI4P consumption, and control of membrane lipid order by endogenous OSBP. EMBO J. 36 (21) e201796687.

Meutiawati, F., Bezemer, B., Strating, J.R.P.M., Overheul, G.J., Žusinaite, E., van Kuppeveld, F.J.M., van Cleef, K.W.R., van Rij, R.P., 2018. Posaconazole inhibits dengue virus replication by targeting oxysterol-binding protein. Antivir. Res. 157 (June), 68–79.

Mimaki, Y., Kuroda, M., Kameyama, A., Sashida, Y., Hirano, T., Oka, K., Maekawa, R., Wada, T., Sugita, K., Beutler, J.A., 1997. Cholestane glycosides with potent cytostatic activities on various tumor cells from ornithogalum saundersiae bulbs. Bioorg. Med. Chem. Lett 7 (5), 633–636.

Nacev, B.A., Grassi, P., Dell, A., Haslam, S.M., Liu, J.O., 2011. The antifungal drug itraconazole inhibits vascular endothelial growth factor receptor 2 (VEGFR2) glycosylation, trafficking, and signaling in endothelial cells. J. Biol. Chem. 286 (51), 44045–44056.

Nchoutmboube, J., Ford-Siltz, L.A., Belov, G.A., 2015. Enterovirus replication: GO with the (Counter)Flow. Trends Microbiol. 23 (4), 183–184.

Pan, G., Cao, X., Liu, B., Li, C., Li, D., Zheng, J., Lai, C., Olkkonen, V.M., Zhong, W., Yan, D., 2018. OSBP-related protein 4L promotes phospholipase Cβ3 translocation from the nucleus to the plasma membrane in jurkat T-cells. J. Biol. Chem. 293 (45), 17430–17441.

Pietrangelo, A., Ridgway, N.D., 2018. Bridging the molecular and biological functions of the oxysterol-binding protein family. Cell. Mol. Life Sci. 75 (17), 3079–3098.

Ridgway, N.D., Dawson, P. a, Ho, Y.K., Brown, M.S., Goldstein, J.L., 1992. Translocation of oxysterol binding protein to Golgi apparatus triggered by ligand binding. J. Cell Biol. 116 (2), 307–319.

Ridgway, N.D., Dawson, P.A., Ho, Y.K., Brown, M.S., Goldstein, J.L., Ridgway, N.D., Dawson, P.A., Ho, Y.K., Brown, M.S., Goldstein, J.L., 2008. Translocation of oxysterol binding protein to Golgi apparatus triggered by ligand binding. 116 (2), 307–319.

Roberts, B.L., Severance, Z.C., Bensen, R.C., Le, A.T., Kothapalli, N.R., Nuñez, J.I., Ma, H.,

Wu, S., Standke, S.J., Yang, Z., et al., 2019. Transient compound treatment induces a multigenerational reduction of oxysterol-binding protein (OSBP) levels and prophylactic antiviral activity. ACS Chem. Biol. 14 (2), 276–287.

Strating, J.R.P.M., van der Linden, L., Albulescu, L., Bigay, J., Arita, M., Delang, L., Leyssen, P., van der Schaar, H.M., Lanke, K.H.W., Thibaut, H.J., et al., 2015Aa. Itraconazole inhibits Enterovirus replication by targeting the oxysterol-binding protein. Cell Rep. 10 (4), 600–615.

Strating, J.R.P.M., van der Linden, L., Albulescu, L., Bigay, J., Arita, M., Delang, L., Leyssen, P., van der Schaar, H.M., Lanke, K.H.W., Thibaut, H.J.J., et al., 2015Ab. Itraconazole inhibits Enterovirus replication by targeting the oxysterol-binding protein. Cell Rep. 10 (4), 600–615.

Tong, J., Yang, H., Yang, H., Eom, S.H., Im, Y.J., 2013Aa. Structure of Osh3 reveals a conserved mode of phosphoinositide binding in oxysterol-binding proteins. Structure 21 (7), 1203–1213.

Tong, J., Yang, H., Yang, H., Eom, S.H., Im, Y.J., 2013Ab. Structure of Osh3 reveals a conserved mode of phosphoinositide binding in oxysterol-binding proteins. Structure 21 (7), 1203–1213.

Wang, H., Ma, Q., Qi, Y., Dong, J., Du, X., Rae, J., Wang, J., Wu, W.-F., Brown, A.J., Parton, R.G., et al., 2019. ORP2 delivers cholesterol to the plasma membrane in exchange for phosphatidylinositol 4, 5-bisphosphate (PI(4,5)P2). Mol. Cell 73 (3), 458–473 e7.

Wong, L.H., Gatta, A.T., Levine, T.P., 2019. Lipid transfer proteins: the lipid commute via shuttles, bridges and tubes. Nat. Rev. Mol. Cell Biol. 20 (2), 85–101.

Yu, W., Jin, Z., 2002. Total synthesis of the anticancer natural product OSW-1. J. Am. Chem. Soc. 124 (23), 6576–6583.

Zhong, W., Pan, G., Wang, L., Li, S., Ou, J., Xu, M., Li, J., Zhu, B., Cao, X., Ma, H., et al., 2016. ORP4L facilitates macrophage survival via G-protein-coupled signaling. Circ. Res. 119 (12), 1296–1312.

Zhong, W., Xu, M., Li, C., Zhu, B., Cao, X., Li, D., Chen, H., Hu, C., Li, R., Luo, C., et al., 2019. ORP4L extracts and presents PIP2 from plasma membrane for PLCβ3 catalysis: targeting it eradicates leukemia stem cells. Cell Rep. 26 (8), 2166–2177 e9.